Forest Ecology and Management 400 (2017) 48–57

Contents lists available at ScienceDirect

Forest Ecology and Management

journal homepage: www.elsevier.com/locate/foreco

Updating national forest inventory estimates of growing stock volume using hybrid inference

Sonia Condés [a,*], Ronald E. McRoberts [b]

[a] Department of Natural Systems and Resources, School of Forest Engineering and Natural Environment, Universidad Politécnica de Madrid, Madrid, Spain
[b] Northern Research Station, U.S. Forest Service, 1992 Folwell Avenue, Saint Paul, MN 55108, USA

ARTICLE INFO

Article history:
Received 30 March 2017
Received in revised form 29 April 2017
Accepted 29 April 2017

Keywords:
Remote sensing
Annual volume change
Annual volume increment
Growth model
Uncertainty

ABSTRACT

International organizations increasingly require estimates of forest parameters to monitor the state of and changes in forest resources, the sustainability of forest practices and the role of forests in the carbon cycle. Most countries rely on data from their national forest inventories (NFI) to produce these estimates. However, because NFI survey years may not match the required reporting years, techniques for updating NFI-based estimates are necessary.

The main aim was to develop an unbiased method to update NFI estimates of mean growing stock volume (m^3/ha) using models to predict annual plot-level volume change, and to estimate the associated uncertainties. Because the final large area volume estimates were based on plot-level model predictions rather than field observations, hybrid inference was necessary to accommodate both model prediction uncertainty and sampling variation. Specific objectives were to compare modelling approaches, to assess the utility of Landsat data for increasing model prediction accuracy, to select the most accurate method, and to compare model-based and design-based uncertainty components. For four monospecific forest types, data from the 2nd and 3rd Spanish NFI surveys together with site variables and Landsat images were used to construct models to predict NFI information for the year of the 4th NFI survey. Data from the 3rd and 4th surveys were used to assess the accuracy of the model predictions at both plot-level and large area spatial scales.

The most accurate method used a set of three models: one to predict the probability of volume removals, one to predict the amount of removed volume, and one to predict gross annual volume. Incorporation of Landsat-based variables in the models increased prediction accuracy. Differences between large area estimates based on plot-level field observations for the 4th NFI survey and estimates based on the model predictions were minimal for all four forest types. Further, the standard errors of the estimates based on the model predictions were only slightly greater than standard errors based on the field observations. Thus, model predictions of plot-level growing stock volume based on field and satellite image data as auxiliary information can be used to update large area NFI estimates for reporting years for which spectral data are available but field observations are not. Finally, variances of means are under-estimated unless hybrid inferential methods are used to incorporate both model prediction uncertainty and sampling variation. For the two forest types for which the two sources of uncertainty were of the same order of magnitude, the under-estimation was non-negligible.

1. Introduction

Recent decades have seen an increasing demand for forest information, at least partially in response to international agreements such as the Kyoto Protocol adopted in 1997. International organizations including the Food and Agriculture Organization of the United Nations (FAO) and the United Nations Framework Convention on Climate Change (UNFCCC) require estimates of the state of and changes in forest resources with the aim of monitoring those

Abbreviations: NFI, National Forest Inventory.

* Corresponding author at: Dept. Sistemas y Recursos Naturales, Escuela Técnica Superior de Ingenieros de Montes, Universidad Politécnica de Madrid, Ciudad Universitaria s/n, 28040 Madrid, Spain.

E-mail address: sonia.condes@upm.es (S. Condés).

http://dx.doi.org/10.1016/j.foreco.2017.04.046
0378-1127/

resources, the sustainability of forest practices and the role of forests in the carbon cycle (Vidal et al., 2016). This increasing demand is reflected not only in the number of parameters for which estimates are requested but also in the increasing frequency of required reports. For example, FAO's Forest Resources Assessment (FRA) assesses the world's forests at 5- to 10-year intervals, while the UNFCCC requires annual reports (Ellis and Moarif, 2015).

National forest inventories (NFI) are the primary sources of information for producing reliable forest-related estimates with associated measures of uncertainty for basic forest attributes of which growing stock volume and forest area are the most common (Tomppo et al., 2010; Vidal et al., 2016). However, because many NFIs were designed with re-measurement cycles longer than the required reporting frequencies, the use of NFI data for responding to the requirements would entail either a revision of NFI protocols (Fridman et al., 2014) or use of prediction techniques to extrapolate NFI-based estimates to the assessment years. As an example, the question of how much woody biomass is available in Europe, which is relevant not only for developing realistic targets for the use of renewable energy sources but also to develop climate change mitigation strategies, is frequently addressed using empirical growth models (Cienciala et al., 2008; Barreiro et al., 2016).

Not all countries, especially those in the Mediterranean region, have well-developed projection systems with models applicable at national scales for all their forest types; more typically the models are restricted to specific species in highly productive regions (Barreiro et al., 2016). Moreover, reliable projections should take into account not only gross annual increment but also additional components such as natural losses and fellings (Tomter et al., 2016). In Europe, fellings are frequently predicted using past estimates of removals or scenario analyses (Salas-González et al., 2001; Barreiro et al., 2016; Tomter et al., 2016) which may or may not accurately reflect future conditions (Nabuurs et al., 2007).

When lengths of inventory re-measurement cycles exceed required reporting frequencies, as is the case for the Spanish NFI (SNFI) for which plots are only re-measured every 10 years, satellite data can be useful for predicting forest changes during the intervening years (González-Alonso et al., 2006). Satellite sensors such as Landsat provide valuable information for a wide variety of ecological applications (Cohen and Goward, 2004). Indices calculated from satellite spectral data have been instrumental in the development of modelling frameworks for detecting harvests (Healey et al., 2006) and forest changes (Hayes and Cohen, 2007) and for estimating biomass and other stand variables (Lu et al., 2004; Boisvenue et al., 2016).

When NFI sample plot data are the only source of forest information, design-based estimators are typically used (Ståhl et al., 2016). Because precision criteria often cannot be satisfied using only sample plot data, auxiliary information in the form of remotely sensed data are frequently used to enhance the estimation process by reducing variances. Common approaches include using models based on a combination of sample plot observations and the remotely sensed auxiliary data to predict an attribute of interest. These model predictions can then be used to construct strata for use with design-based, stratified estimators or they can be used directly with design-based, model-assisted regression estimators (McRoberts, 2010; McRoberts et al., 2013).

When observations for the sample plot locations for the time period of interest are not available, models are used to predict forest attributes for those locations. For such cases, uncertainties associated with the model predictions should be incorporated to ensure that the variance estimators are unbiased. Failure to acknowledge and incorporate the uncertainties associated with the model predictions is not uncommon, but of necessity leads to under-estimating the variances of population parameters, which may lead to poor decisions. Methods for incorporating uncertainty from both modelling and sampling sources into variance estimators for population parameters are characterized as *hybrid inference* (Corona et al., 2014; McRoberts et al., 2016; Ståhl et al., 2016). The primary features of hybrid inference are a probability sample of population units, but model predictions rather than observations for the attribute of interest for those sample units. The models are typically constructed using data either external to the spatial region of the sample or, in the case of updating NFI estimates, external to the temporal timeframe of the sample. Characterization of these methods as hybrid inference arises from the need to use model-based inferential techniques to estimate the component of uncertainty due to the use of model predictions rather than observations, and design-based inferential techniques to estimate the uncertainty component due to probability sampling rather than conducting a complete census of the population.

The primary objective of the study was to develop an unbiased method for updating estimates of NFI mean growing stock volume (m^3/ha) using models based on data from previous inventory cycles to predict annual plot-level volume change, and to estimate the associated uncertainties. The framework for the study was hybrid inference to accommodate both the model-based and design-based inferential components. Multiple prediction methods based on field, climatic, topographic, and Landsat-based independent variables were used to predict annual volume change, ΔV. The specific technical objectives were i) to compare multiple updating methods with respect to both plot-level prediction accuracy and large area estimates of future mean growing stock volume and to select the most accurate method, ii) to assess the utility of Landsat data for increasing model prediction accuracy and the precision of the population parameter estimator, and iii) to compare the relative magnitudes of the model-based and design-based uncertainty components.

2. Materials and methods

2.1. Data

2.1.1. Sample plot data

From its 2nd survey beginning in 1986, the Spanish National Forest Inventory (SNFI) has been a continuous inventory featuring a systematic sample of permanent plots located at the nodes of a 1-km square grid and remeasured using an approximate 10-year inventory cycle. Sample plots are concentric with 5-, 10-, 15- and 25-m radii for which diameters and heights of all trees with breast-height diameters of at least 7.5, 12.5, 22.5 and 42.5 cm, respectively, are measured. Allometric models are used to predict individual tree volumes which are weighted to accommodate the different concentric plot radii to predict total plot growing stock volume and aggregated to produce plot-level growing stock volume estimates.

The analyses focused on four monospecific forest types located in two Regions of Spain where the 2nd, 3rd and 4th SNFI surveys have been completed (Table 1): *Pinus halepensis* Mill. in the Region of Murcia and *Fagus sylvatica* L., *Pinus sylvestris* L. and *Pinus radiata* D. Don in País Vasco (Fig. 1).

2.1.2. Auxiliary site data

For each plot, topographic slope (Slp, degrees) obtained from 1:25,000 topographic maps in raster format (IGN, 2003) was used as a measure of terrain conditions. Mean annual temperature (T, °C) and annual precipitation (P, mm) were obtained from raster maps with a 1-km resolution for the Iberian Peninsula (Gonzalo Jiménez, 2010). The Martonne aridity index (Martonne, 1926) was calculated as $M = P/(T + 10)$ and was used as a measure of

Table 1
SNFI field work years and Landsat image acquisition dates.

	SNFI's cycle	Field work	Landsat images Path	Row	Sensor	Acquisition date
País Vasco	2nd	1996			ETM+	05/09/1999
	3rd	2005	201	30	TM	24/09/2003
	4th	2011			TM	26/06/2011
Murcia	2nd	1987	199	33	TM	26/06/1987
	3rd	1999	199	34	ETM+	21/07/1999
	4th	2010			TM	11/07/2010

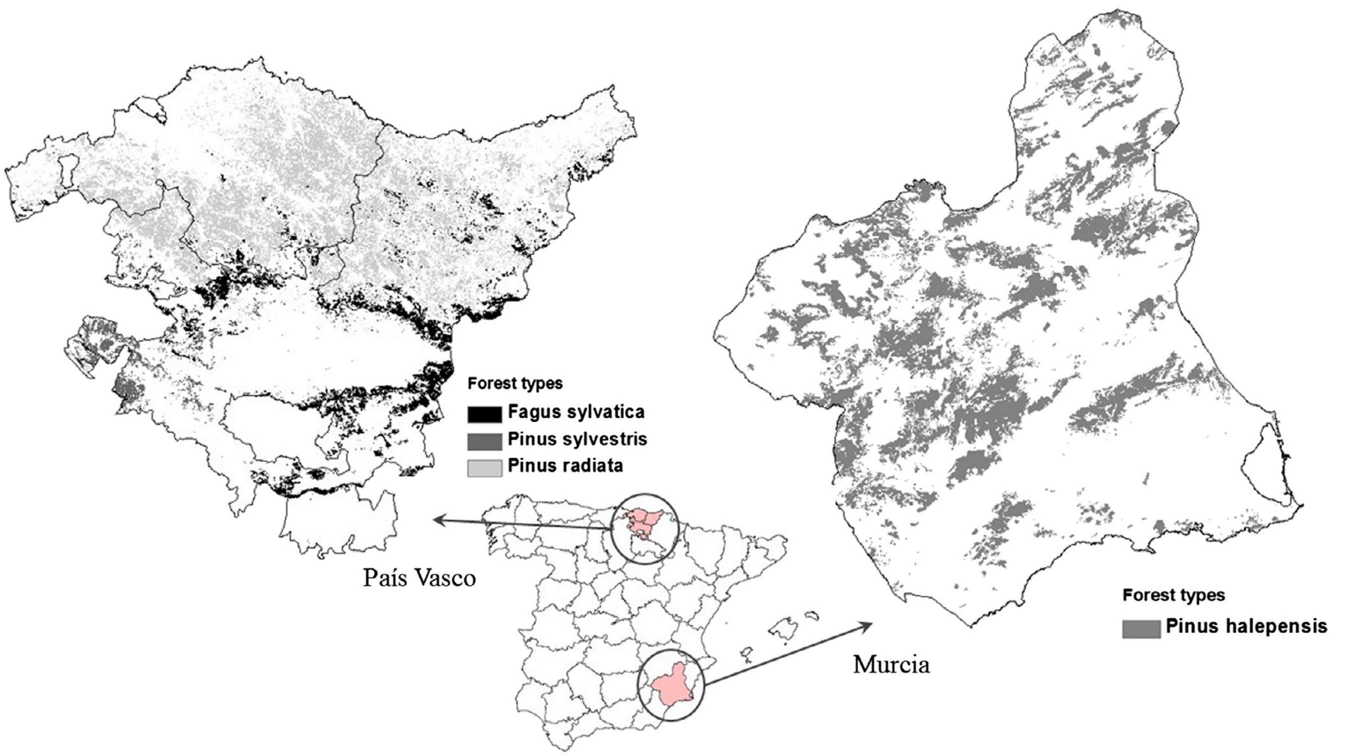

Fig. 1. Location of the forest types in Spain.

climatic conditions. All auxiliary site data were assumed to remain constant over time.

2.1.3. Auxiliary remotely sensed data

Landsat imagery corresponding to the years of the SNFI surveys were used, although image and plot measurement dates differed slightly for the País Vasco Region because of image unavailability and the failure of the Landsat scan line corrector (Table 1). All Landsat imagery was radiometrically calibrated, atmospherically and topographically corrected, and areas with cloud cover were removed (Goslee, 2011). For atmospheric correction, the modified dark object subtraction method introduced by Song et al. (2001) was used. Topographic correction used the C-correction method (Teillet et al., 1982) with the slope smoothing as recommended by Riaño et al. (2003).

Multiple vegetation indices that have been reported as useful for forest studies were calculated from the Landsat spectral responses for years corresponding to the SNFI surveys (Lu et al., 2004; Hall et al., 2006; Healey et al., 2006). However, preliminary analyses indicated strong multicollinearity among the spectral measures. Therefore, only the two indices most correlated with both volume increment and volume removals were used: band 5 (B5), and the normalized vegetation index (NDVI) (Tucker, 1979).

2.1.4. Datasets

For each forest type, two datasets were constructed. *Dataset 2–3* consisted of the plot-level volume observations, auxiliary site data, and both Landsat B5 and NDVI for plots measured in both the 2nd and 3rd SNFI surveys. In addition, for each sample plot j, the annual observed volume change ΔV_{23j} was calculated. Further, as per Martin (1982), the volume changes were disaggregated into the gross annual volume increment, IV_{23j} ($\mathrm{m^3\,ha^{-1}\,year^{-1}}$) and total volume removals between the two SNFI surveys, VR_{23j}, ($\mathrm{m^3\,ha^{-1}}$), due to both natural losses and felling:

$$\Delta \mathrm{V}_{23j} = \frac{V_{3j} - V_{2j}}{\Delta t_{23}} = \mathrm{IV}_{23j} - \frac{VR_{23j}}{\Delta t_{23j}} \qquad (1)$$

where V_{2j} and V_{3j} were the observed volumes for plot j at the 2nd and 3rd SNFI surveys, and Δt_{23} is the number of years between surveys. Data for the $j = 1, \ldots, n_{23}$ plots represented in dataset 2–3 were used to construct models for predicting volume change using one of the five methods described in Section 2.3.

Dataset 3–4 was constructed in the same manner as dataset 2–3, except all data corresponded to the 3rd and 4th SNFI surveys instead of the 2nd and 3rd SNFI surveys. Models constructed using dataset 2–3 were applied to data for the $j = 1, \ldots, n_{34}$ plots represented in dataset 3–4. In particular, the data from dataset 3–4 to which the models were applied were plot-level data from the 3rd SNFI survey, auxiliary site data which did not change between surveys, and Landsat B5 and NDVI for years corresponding to both the 3rd and 4th SNFI surveys. The models and the dataset 3–4 data were used to predict volume changes $\widehat{\Delta V}_{34j}$ and the corresponding updated plot-level volume estimates, $\hat{V}_{4j}$, from the plot-level observations for the same plots for the 3rd SNFI, V_{3j}:

$$\hat{V}_{4j} = V_{3j} + \widehat{\Delta V}_{34j} \cdot \Delta t_{34j}, \tag{2}$$

where Δt_{34j} is the number of year between the 3rd and 4th SNFI survey re-measurements for plot j. Dataset 3–4 was also used for validating the results by comparing predicted plot-level volumes with corresponding observations for 4th SNFI. In addition, large area estimates based on the model predictions were compared to similar estimates based on 4th SNFI plot-level observations. Of importance, although data from the 3rd SNFI cycle were included in both dataset 2–3 and dataset 3–4, some plots represented in dataset 2–3 were not represented in dataset 3–4 and vice versa. The differences were larger for the forest types in the País Vasco Region, where about the 80% of plots in dataset 3–4 were represented in dataset 2–3 but about the 50% of plots in dataset 2–3 were not represented in dataset 3–4. For the Murcia Region the plots differing between datasets were less than 10%. This was a consequence of changes in forest lands, difficulties in locating the permanent sample plots established during previous NFIs cycles and, in the case of the País Vasco Region, budget problems due the economic crisis that forced reduction in the number of sample plots during the 4th SNFI. Plot information for the four forest types is summarized in Table 2.

2.2. Hybrid inference for mean growing stock

When only model predictions rather than observations are available, unbiased variance estimators of population parameters must incorporate the uncertainty of the model predictions. Hybrid inference is increasingly recognized as the statistically correct approach for estimating the variances of population parameters under this condition. Four key features characterize hybrid inference: (1) a probability sample of population units for which only auxiliary information, not observations of the response variable, are available; (2) a model based on the auxiliary information to predict the response variable for the sample units; (3) a design-based estimator of the population parameter using the model predictions for the sample units; and (4) both model-based and design-based inferential methods to estimate the variance of the population parameter estimator. For this study, the probability sample consisted of the plot locations for the 4th SNFI survey; the auxiliary information included dataset 2–3, the site data, and Landsat B5 and NDVI; the models were as described in Section 2.3; and both the model-based and design-based inferential methods were incorporated into variance estimators as described below.

For each forest type, the mean population volume for the 4th SNFI survey was estimated using predicted volumes $\hat{V}_{4j}$ obtained using Eq. (2) as:

$$\hat{\mu}_4 = \frac{\sum \hat{V}_{4j}}{n_{34}} = \frac{1}{n_{34}} \sum_{j=1}^{n_{34}} (V_{3j} + \widehat{\Delta V}_{34j} \cdot \Delta t_{34j}), \tag{3}$$

Methods for predicting $\widehat{\Delta V}_{34j}$ are described in Section 2.3. Of importance, because data for the 4th SNFI survey were assumed to be as yet unavailable, $\widehat{\Delta V}_{34j}$ had to be predicted using data from previous SNFI surveys.

An unbiased estimator of the variance of $\hat{\mu}_4$, $Var(\hat{\mu}_4)$, must incorporate uncertainty from three sources: (i) the uncertainty due to using model predictions, $\widehat{\Delta V}_{34j}$, rather than observations, ΔV_{34j}, for volume change between the 3rd and 4th SNFI surveys, (ii) the uncertainty due to using a probability sample rather than a complete census of the population for the 4th SNFI cycle, and (iii) the covariance between estimates for the first two sources as a result of using at least some of the same plots as sources of data for constructing the models as were used to apply the models, although the data for the two purposes were acquired at different times.

Because of the complexities involved with estimation of the three uncertainty components, a replicated Monte Carlo bootstrap

Table 2
Summary of the SNFI data.

		Dataset 2–3: Plots re-measured in 2nd and 3rd SNFI's cycles				Dataset 3–4: Plots re-measured in 3rd and 4th SNFI's cycles				
		V_2	VR_{23}	IV_{23}	ΔV_{23}	V_3	VR_{34}	IV_{34}	ΔV_{34}	V_4
Fagus sylvatica	n		299					178		
	mean	140.7	8.0	4.2	3.4	171.3	6.9	3.8	2.6	186.9
48,248 has	sd	80.9	20.6	2.9	3.9	94.7	16.8	2.8	3.9	99.2
	min	0.0	0.0	−0.6	−16.8	5.6	0.0	−0.8	−19.5	1.2
	max	407.3	154.9	17.6	17.6	478.3	137.1	11.6	11.3	540.1
Pinus sylvestris	n		105					65		
	mean	124.0	9.6	4.6	3.5	158.6	10.0	4.3	2.6	174.3
15,365 has	sd	76.2	18.4	3.7	4.2	96.6	24.8	3.1	4.9	96.0
	min	2.3	0.0	0.4	−8.0	15.7	0.0	0.8	−20.5	21.7
	max	397.1	90.5	16.6	15.3	474.0	141.4	14.2	11.8	449.1
Pinus radiata	n		609					474		
	mean	154.1	31.3	14.9	11.5	207.0	42.4	15.2	8.1	255.6
129,062 has	sd	157.9	66.4	8.3	11.9	173.1	100.2	9.0	21.7	181.6
	min	0.0	0.0	0.0	−63.3	0.0	0.0	−0.6	−141.9	0.0
	max	896.6	569.6	44.1	43.7	878.2	851.3	56.4	53.1	925.6
Pinus halepensis	n		909					945		
	mean	18.6	2.6	0.8	0.6	26.2	2.3	1.0	0.8	35.2
246,512 has	sd	19.9	8.2	1.0	1.1	25.2	6.8	1.0	1.1	29.7
	min	0.0	0.0	−0.8	−8.0	0.0	0.0	−0.7	−4.4	0.0
	max	131.3	111.2	6.5	6.1	143.8	72.4	4.7	4.7	181.1

V_2, V_3 and V_4 – volume (m^3/ha) at 2nd, 3rd and 4th SNFI's cycles respectively, VR_{23} and VR_{34} – volume removals (m3/ha), IV_{23} and IV_{34}– Gross volume increments (m3/(ha·year)), ΔV_{23} and ΔV_{34}– Annual volume change (m3/(ha·year)) between 2nd and 3rd SNFI's cycles and between 3rd and 4th SNFI's cycles, respectively. n – Number of plots represented in each dataset.

approach (Efron and Tibshirani, 1994), similar to that described by McRoberts et al. (2016), was used to estimate $Var(\hat{\mu}_4)$. For each replication, r = 1, . . . , 10,000, a bootstrap resample the same size as the original sample was randomly drawn with replacement from dataset 2–3. The models were refit to the data from each bootstrap resample of dataset 2–3 and applied to a bootstrap resample of dataset 3–4 which was also same size as the original 4th SNFI survey sample but randomly drawn with replacement. For each replication, an estimate $\hat{\mu}_4^r$ was obtained. The overall bootstrap estimator of the population mean was,

$$\hat{\mu}_4 = \frac{\sum_{j=1}^{10,000} \hat{\mu}_4^r}{10,000}, \tag{4}$$

with variance estimator as,

$$\widehat{Var}(\hat{\mu}_4) = \frac{\sum_{j=1}^{10,000} (\hat{\mu}_4^r - \hat{\mu}_4)^2}{10,000}. \tag{5}$$

Graphs of the bootstrap estimates of the means and variances versus number of replications showed that 10,000 replications were sufficient for the estimates of both the means and the variances to stabilize.

An estimate of the uncertainty due to the modelling component was estimated separately by using bootstrap resamples from dataset 2–3 to refit the models but using only the original dataset 3–4 when applying the models. Similarly, an estimate of the uncertainty due to the sampling component was estimated separately by using only the original dataset 2–3 to fit the models but using bootstrap resamples of dataset 3–4 when applying the models.

2.3. Methods for predicting annual volume changes

Five methods were used to predict annual, plot-level, volume change for years subsequent to the year of the last NFI field work.

2.3.1. Mean annual volume change for the previous SNFI cycle

The first method for predicting volume change was the method currently used by the SNFI. For each forest type, annual plot-level volume changes $\widehat{\Delta V}_{34}$ were predicted using the mean of the observed volume changes, $\overline{\Delta V}_{23}$, over all permanent plots measured for both the 2nd and 3rd SNFI cycles:

$$\widehat{\Delta V}_j = \overline{\Delta V}_{23} = \frac{1}{n_{23}} \sum_{j=1}^{n_{23}} \frac{(V_{3j} - V_{2j})}{\Delta t_{23}} \tag{6}$$

Note that the $j = 1, \ldots, n_{23}$ plots represented in dataset 2–3 used for estimating mean annual volume change could be different than the plots represented in dataset 3–4 to which the mean is used as a prediction of annual plot-level change. This approach was designated *method A*.

2.3.2. Annual volume change models

The second method for predicting annual plot-level volume change between the years t and $t + \Delta t$ used simple linear models constructed using data for the previous two SNFI surveys:

$$\Delta V_j = a_0 + a_1 \mathrm{G}_{tj} + a_2 \mathrm{Ho}_{tj} + a_3 dg_{tj} + a_4 Slp_j + a_5 M_j + \varepsilon_j \tag{7}$$

where G_t, Ho_t and dg_t were respectively plot basal area ($\mathrm{m}^2\ \mathrm{ha}^{-1}$), dominant height (m), and quadratic mean diameter (cm), for the first of the two surveys, Slp was topographic slope (degrees) and M was the Martonne aridity index, the latter two of which were assumed to be constant over time, and $a_1, \ldots, a_5$ were coefficients to be estimated. This approach was designated *method B*.

With the aim of improving model prediction accuracy, variables obtained from the Landsat spectral data were also considered as predictors. Because years for the SNFI field work and the Landsat imagery differed for some forest types (Table 1), Landsat B5 and NDVI for both the first and last years of the SNFI cycles were considered separately as independent variables rather than as band differences or ratios. This approach using linear models and spectral response variables was designated *method B + L*.

Models were fit using plot data for dataset 2–3. Independent variables were incorporated into the model if they statistically significantly improved the quality of fit of the model as assessed at the $\alpha = 0.05$ significance level using the F-test based on the extra sum of squares principle (Ratwosky, 1983). The models were then applied to data for plots represented in dataset 3–4 to predict annual plot-level volume change. Adjusted R^2, denoted R^2_{adj}, is a modification of R^2 that accounts for the number of predictor variables and was used as a measure of the goodness of fit of the models to the data. Note that, unlike R^2, R^2_{adj} may decrease when an additional predictor variable is included in the model.

2.3.3. Annual volume increment and volume removals models

The third method used a set of multiple models for each forest type to predict gross annual volume increment IV_j and total volume removals VR_j between year t and $t + \Delta t$:

$$\begin{aligned} \log(IV_j + 1) = {} & a_0 + a_1 \log(\mathrm{G}_{tj} + 1) + a_2 \log(\mathrm{Ho}_{tj} + 1) \\ & + a_3 \log(dg_{tj} + 1) + a_4 Slp_j + a_5 M_j + \varepsilon_j, \end{aligned} \tag{8}$$

Because of the large number of zero-valued observations for VR_j, a condition characterized as zero inflation, this variable was predicted in two steps. First, a logistic model for the probability of a removal greater than 0, $P_{VR>0}$, was constructed as:

$$\begin{aligned} \mathrm{logit}(P_{VR>0}) = {} & a_0 + a_1 \log(\mathrm{G}_{tj} + 1) + a_2 \log(\mathrm{Ho}_{tj} + 1) \\ & + a_3 \log(dg_{tj} + 1) + a_4 Slp_j + a_5 M_j + \varepsilon_j, \end{aligned} \tag{9}$$

and, second, a linear model for the volume removed was constructed as:

$$\begin{aligned} \log(VR_j) = {} & a_0 + a_1 \log(\mathrm{G}_{tj}) + a_2 \log(\mathrm{Ho}_{tj}) + a_3 \log(dg_{tj}) \\ & + a_4 Slp_j + a_5 M_j + \varepsilon_j \end{aligned} \tag{10}$$

The models of Eqs. (8) and (9) were fit using data for all plots represented in dataset 2–3, whereas the model of Eq. (10) was fit using only the subset of plots with removals greater than 0. Natural logarithmic transformations of the original variables were necessary to normalize distributions of residuals and to reduce heteroscedasticity. When transforming back to the original scales, the bias induced by the logarithmic transformation was corrected using the Beauchamp and Olson (1973) coefficient.

As previously, the statistical significance of the contributions of independent variables for increasing the quality of fit of the models to the data was assessed at the $\alpha = 0.05$ significance level. R^2_{adj} and Nagelkerke-R^2 (Nagelkerke, 1991) were used as measures of quality of fit for the linear and logistic models, respectively. For future reference, this approach is designated *method C*.

In the same manner as for method B, the Landsat B5 and NDVI variables were considered for use as independent variables. In this case B5 corresponding to both the first and last years of the respective SNFI cycles, was used as a predictor of removals (Eqs. (9) and (10)) while NDVI, also for the first and last years of cycles, was used as predictor of annual volume increment (Eq. (8)). This approach was designated *method C + L*.

The models were applied to data for plots represented in dataset 3–4 to predict annual plot-level volume change as:

$$\widehat{\Delta V}_j = \widehat{IV}_j \cdot \Delta \mathrm{t}_j - \widehat{VR}_j, \tag{11}$$

where the volume removals $\widehat{VR}_j$ were 0 for plots with predicted probability $P_{VR>0}$ less than 0.5 (Eq. (9)) and estimated with Eq. (10) for the other plots.

2.4. Model prediction accuracy

The accuracies of the prediction methods were assessed at two levels. First, a plot-level assessment was based on residuals calculated for each plot, j, as the difference between $V_{4\,j}$ and $\hat{V}_{4\,j}$ where $\hat{V}_{4\,j}$ is obtained using one of the methods described in Section 2.3. The distributions of residuals were summarized for each forest type and method using mean error (ME), mean absolute error (MAE) and root mean square error (RMSE):

$$ME = \frac{\sum_{j=1}^{n}(\hat{V}_{4j} - V_{4j})}{n_{34}}, \tag{12}$$

$$MAE = \frac{\sum_{j=1}^{n}|\hat{V}_{4j} - V_{4j}|}{n_{34}}, \tag{13}$$

and

$$RMSE = \sqrt{\frac{\sum_{j=1}^{n}(\hat{V}_{4j} - V_{4j})^2}{n_{34} - 1}} \tag{14}$$

where n_{34} is the number of sample plots represented in dataset 3–4 within the forest type. Note that ME, MAE and RMSE were calculated using dataset 3–4, not dataset 2–3 which was used to construct and fit the models.

Second, inferences for estimates of μ_4 in the form of a confidences intervals were calculated as $\hat{\mu}_4 \pm t_{1-\alpha} SE(\hat{\mu}_4)$, where the standard error was calculated as $SE(\hat{\mu}_4) = \sqrt{\widehat{Var}(\hat{\mu}_4)}$. Although model prediction accuracy is important, the models are just intermediate steps enroute to the inference. Therefore, for each forest type and method, confidence intervals at the 0.95 significance level were also calculated for $\hat{\mu}_4$. The confidence interval half-widths as expressed by $t_{1-\alpha} \cdot SE(\hat{\mu}_4)$ were compared as means of assessing the relative accuracies of the prediction techniques. In addition, the confidence interval based on just the 4th SNFI plot observations was calculated as a means of assessing the degree to which precision is lost by using model predictions, $\hat{V}_{4j}$, rather than observations, V_{4j}, when estimating μ_4. Finally, uncertainties due to the modelling and sampling components were compared using their respective standard errors: $SE_M(\hat{\mu}_4)$ and $SE_D(\hat{\mu}_4)$.

3. Results

3.1. Model prediction accuracy

3.1.1. Model prediction accuracy for the calibration data (dataset 2–3)

In general, inclusion of the Landsat variables B5 and NDVI in the B + L and C + L models produced an increase in R^2_{adj}. For the annual volume change models (Eq. (7)), method B produced only small R^2_{adj} values, ranging from 0.0065 for *Pinus radiata* to 0.2414 for *Pinus sylvestris* (Supplementary Table 1), but always increasing when the Landsat variables were incorporated. For the broadleaf forest type, Fagus sylvatica, the increase due to the Landsat variables was very slight although statistically significant. For this forest type, only the Landsat variables for the 2nd NFI survey contributed to statistically significantly improving the quality of fit of the model to the data with the result that no Landsat variables representing the final conditions were included in the model. For the other forest types, the increase in R^2_{adj} when including Landsat variables was between 0.10 and 0.15 which, although small in absolute terms, still represented a large relative increase.

For method C, the Landsat variables that contributed to statistically significantly improving the fit of the models differed by forest type (Supplementary Tables 2–4). For the annual volume increment models of Eq. (8), the models for all forest types included NDVI for the 2nd NFI, for the 3rd NFI or both. For the logistic models of Eq. (9), B5 was included in the model only for *Fagus sylvatica* and *Pinus halepensis*. For volume removals models of Eq. (10), only the models for *Pinus radiata* and *Pinus halepensis* included the B5 variable.

The contributions of the Landsat variables were especially remarkable for models for the *Pinus halepensis* forest type for which the Landsat acquisition dates and the years for which SNFI field work were conducted matched closely. For this forest type, Landsat variables for both the first and final year of the SNFI cycle always contributed to statistically significantly increasing the quality of fit of the models to the data. R^2_{adj} for the logistic model of Eq. (9) increased from 0.23 to 0.41 and produced an increase in accuracy from 79% to 84% for distinguishing plots without and with removals. For the volume removal model of Eq. (10) R^2_{adj} increased from 0.19 to 0.42.

3.1.2. Model prediction accuracy for the accuracy assessment data (dataset 3–4)

Table 3 summarizes the analysis of residuals for each forest type resulting from applying the models to dataset 3–4. It has to be noticed that, while the accuracy analysed in the last section referred to annual volume changes, this table refers to mean errors calculated for predicted volumes according Eq. (2). Therefore, the small values of R^2_{adj} reported for the volume change models were more important when calculating ME, MAE and RMSE for the forest types with the greater values of volume increment and volume removals as *Pinus radiata* (Table 2).

For all forest types, ME was greater for method A than for methods B and C. In addition, ME was always nearer 0 for methods B + L and C + L which included the Landsat variables than for methods B and C. Overall, method C + L produced the smallest MEs. In general, for all forest types, methods B + L and C + L produced smaller MAEs and RMSEs than the corresponding methods B and C. However, for the *Fagus sylvatica* forest type, RMSE was 0.2 m^3/ha greater for method B + L than for method B; similar results were observed for *Pinus halepensis* for which MAE and the RMSE were 0.6 and 0.3 m^3/ha greater, respectively, for method B + L than for method B. Also, for *Pinus radiata*, MAE was 1.2 m^3/ha greater for method C + L than for Method C, despite the clear reductions in ME and RMSE. For purposes of clarification, we note that greater ME, MAE, or RMSE for methods B + L or C + L than for B or C is possible because the model was constructed for dataset 2–3 but applied to dataset 3–4.

3.2. Inference

Population estimates of the mean ($\hat{\mu}_4$) and standard error $SE(\hat{\mu}_4)$ together with the components $SE_D(\hat{\mu}_4)$ and $SE_M(\hat{\mu}_4)$, are reported in Table 4. When comparing confidence intervals at the $1 - \alpha = 0.95$ confidence level, estimates of means for *Pinus radiata and Pinus halepensis* obtained with method A were outside the confidence interval constructed using only observations, V_{4j}, and simple random sampling estimators (Fig. 2). Further, method C + L produced confidence intervals that were most similar to the latter confidence intervals although the SEs were slightly greater.

In general, for all forest types, the largest values of $SE(\hat{\mu}_4)$ were for methods B + L and C + L which included Landsat variables (Table 4), although the differences relative to the other methods

Table 3
Accuracy measures based on plot-level residuals between the observed and predicted volume for the 4th SNFI for the five methods described in Section 2.3.

Modeling approach	Fagus sylvatica (178 plots)			Pinus sylvestris (65 plots)		
	ME	MAE	RMSE	ME	MAE	RMSE
A	4.6	16.7	23.2	5.5	18.2	29.5
B	6.0	16.8	23.0	5.4	20.6	33.2
B + L	3.5	16.1	23.2	−1.1	20.3	32.6
C	2.3	16.6	23.5	−0.3	20.3	31.3
C + L	0.4	16.4	23.5	0.0	20.2	30.1
	Pinus radiata (474 plots)			Pinus halepensis (945 plots)		
	ME	MAE	RMSE	ME	MAE	RMSE
A	20.2	71.0	129.9	−2.2	8.6	11.9
B	18.5	70.7	128.7	−1.5	8.0	11.5
B + L	4.2	70.3	124.5	−0.4	8.6	11.8
C	13.0	71.5	128.2	−1.4	8.8	12.4
C + L	1.6	72.7	123.8	0.0	8.6	11.9

Table 4
Estimates of mean volume, $\hat{\mu}_4$, and standard errors, $SE(\hat{\mu}_4)$, for the four forest types and five methods described in Section 2.3.

	Fagus sylvatica (186 plots)[a]				
	$\hat{\mu}_4$	ME	$SE_M(\hat{\mu}_4)$	$SE_D(\hat{\mu}_4)$	$SE(\hat{\mu}_4)$
Observed	186.9	–	0.0	7.4	7.4
A	191.4	4.6	1.4	7.1	7.2
B	192.8	6.0	1.5	7.3	7.4
B + L	190.3	3.5	1.8	7.4	7.6
C	189.2	2.3	2.3	7.1	7.4
C + L	187.3	0.4	2.3	7.1	7.4
	Pinus sylvestris (65 plots)				
	$\hat{\mu}_4$	ME	$SE_M(\hat{\mu}_4)$	$SE_D(\hat{\mu}_4)$	$SE(\hat{\mu}_4)$
Observed	174.3	–	0.0	11.9	11.9
A	179.8	5.5	2.4	12.0	12.1
B	179.6	5.4	2.1	12.5	12.5
B + L	173.2	−1.1	3.3	12.6	12.9
C	173.9	−0.3	3.8	12.0	12.4
C + L	174.3	0.0	3.7	11.5	12.0
	Pinus radiata (474 plots)				
	$\hat{\mu}_4$	ME	$SE_M(\hat{\mu}_4)$	$SE_D(\hat{\mu}_4)$	$SE(\hat{\mu}_4)$
Observed	255.6	–	0.0	8.3	8.3
A	275.7	20.2	2.9	8.0	8.5
B	274.1	18.5	3.5	7.8	8.5
B + L	259.8	4.2	5.2	7.9	9.5
C	268.6	13.0	4.6	7.5	8.8
C + L	257.2	1.6	5.6	7.5	9.4
	Pinus halepensis (945 plots)				
	$\hat{\mu}_4$	ME	$SE_M(\hat{\mu}_4)$	$SE_D(\hat{\mu}_4)$	$SE(\hat{\mu}_4)$
Observed	35.2	–	0.0	1.0	1.0
A	33.0	−2.2	0.4	0.8	0.9
B	33.7	−1.5	0.5	0.9	1.0
B + L	34.8	−0.4	0.8	0.8	1.1
C	33.8	−1.4	0.8	0.8	1.1
C + L	35.2	0.0	0.7	0.8	1.1

[a] $SE_M(\hat{\mu}_4)$ is the standard error corresponding to the model prediction uncertainty, and $SE_D(\hat{\mu}_4)$ is the standard error corresponding to sampling variation; and is the ME the mean error used as an estimate bias for $\hat{\mu}_4$.

were small. For instance, when comparing values of $SE(\hat{\mu}_4)$ for method B + L with values obtained using the 4th SNFI survey observations, differences were small, ranging between 0.2 m^3/ha for *Fagus sylvatica* and 1.2 m^3/ha for *Pinus radiata*. Further, $SE(\hat{\mu}_4)$ for method C + L was always smaller than for method B + L, although always larger than $SE(\hat{\mu}_4)$ obtained using the 4th SNFI survey observations.

When analyzing the component of uncertainty due to modelling, method A produced the smallest $SE_M(\hat{\mu}_4)$ among all forest types. However, methods with the smallest SEs also produced the greatest MEs. Moreover, methods B + L and C + L that included Landsat variables had the smallest MEs but the greatest values of $SE(\hat{\mu}_4)$, primarily as a consequence of greater values for $SE_M(\hat{\mu}_4)$.

Regardless of the method used to update volume estimates, failure to incorporate the component of uncertainty due to using model predictions rather than observations of annual plot-level volume change of necessity led to systematic under-estimation of the SEs. This under-estimation was more important for the forest types *Pinus radiata* or *Pinus halepensis* for which the numbers of sample plots used in this study were larger. For these forest types, $SE_M(\hat{\mu}_4)$ and $SE_D(\hat{\mu}_4)$ were of same order of magnitude (Table 4) which exacerbates the consequences of failing to incorporate the

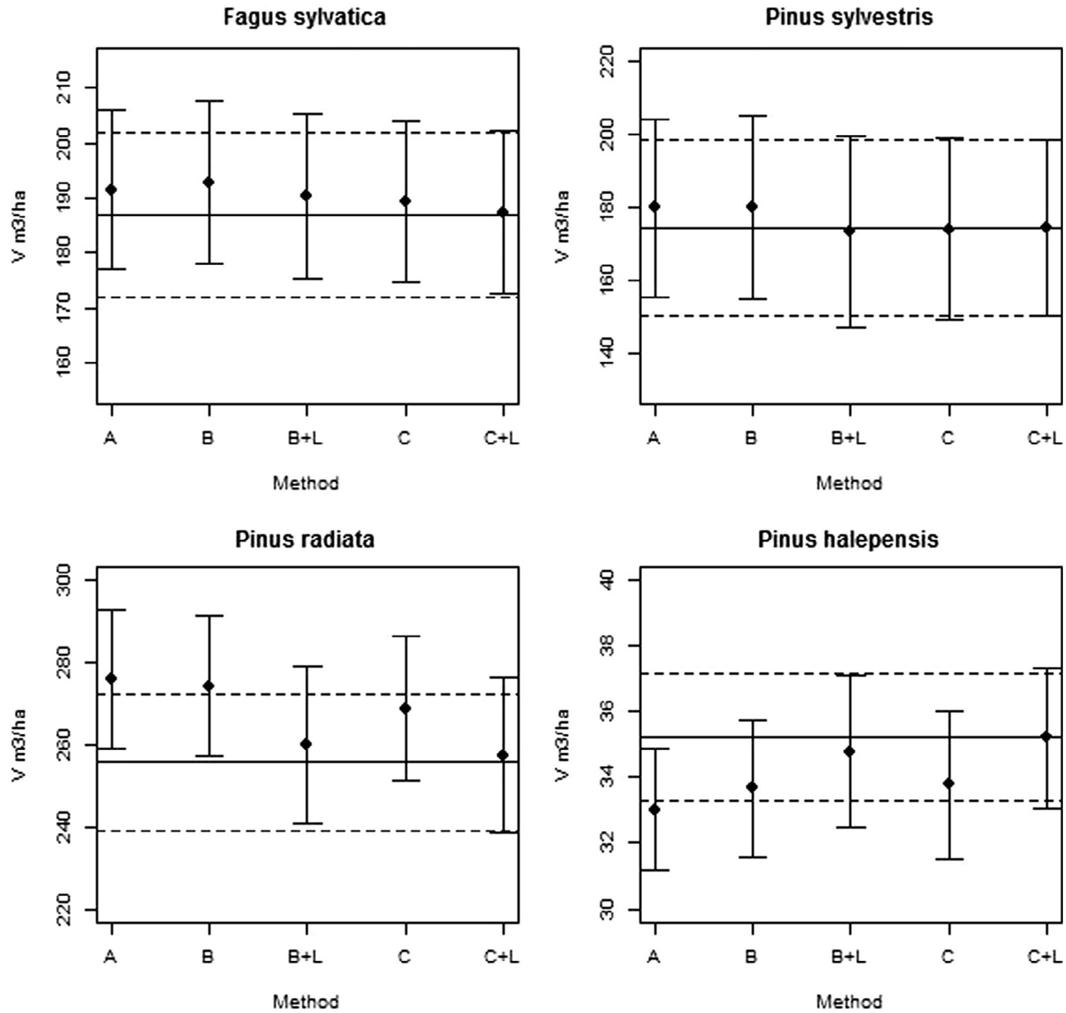

Fig. 2. Confidence intervals at α = 0.05 significance level for the mean volume estimates for the four forest types and five methods described in Section 2.3. The solid and dashed horizontal lines are the mean and lower and upper bounds, respectively, for a confidence interval for mean volume based on the 4th SNFI plot observations. Note that OY axis has different scales.

uncertainty associated with the model predictions when estimating variances. The ratio of the half-width of the confidence interval and the estimate of the mean, expressed as a percentage,

$$HW = \frac{t_{1-\alpha}SE(\hat{\mu}_4)}{\hat{\mu}_4}, \tag{15}$$

can be used as a measure of relative estimated precision. For the most accurate prediction method, C + L, correctly incorporating the uncertainty due to using model prediction increased relative HW% from 5.8% to 7.3% for *Pinus radiata* and from 4.6% to 6.1% for *Pinus halepensis*.

4. Discussion

4.1. Models

The main objective of the study was to develop an unbiased method for updating growing stock volume estimates which, together with their corresponding uncertainties, could be used to respond to questionnaires from the international forest assessments for years between NFI field measurements. Simple models developed using data from NFI sample plots measured in previous surveys produced updated estimates that were similar to estimates based on field plot observations. Of importance, these models are only appropriate for short-term predictions for which growth conditions such as climate and management regimes are expected to be stable (Peng, 2000).

Moreover, future European harvest rates are expected to increase by as much as 30% relative to 2010 estimates (Barreiro et al., 2016). This situation increases the importance of using models that incorporate some current conditions to update growing stock rather than simply using past volume change measurements as is the case for method A. This issue is even more crucial for fast-growing species such as the *Pinus radiata*. Method C + L, which explicitly predicts removals, was the most accurate at both the plot and population levels.

Inclusion of satellite image-based independent variables in the prediction models presented challenges. Although Landsat data have been widely used to assess forest area, structure, harvest, and growing stock volume (Lu et al., 2004; Hall et al., 2006), few studies have reported the use of Landsat data as independent variables in change models for these attributes other than those related to area (e.g., Suratman et al., 2004). Further, the accuracies of few such models have been assessed using new datasets for purposes of forecasting future conditions. In this sense, we found that inclusion of Landsat variables corresponding to the prediction year generally increased the accuracy of model predictions as measured by R^2_{adj} when assessed for dataset 2–3. However, this increase did not always produce more accurate plot-level volume model predictions when the models were applied to dataset 3–4; in fact, for

Fagus sylvatica and *Pinus halepensis* using method B and for *Pinus radiata* using method C, MAE and/or RMSE were actually larger (Table 3). However, because there is widespread general consensus that unbiased estimators are preferred, even if associated variances are somewhat larger, for this study we regarded ME as more important than MAE, RMSE or uncertainty.

An important benefit of methods B + L and C + L is the possibility of including Landsat variables as predictors, not only for the first year of an SNFI cycle, as is the case for field variables, but also for the last year of the cycle. This feature potentially circumvents the necessity of detailed scenario analyses, detailed records of thinning, and accommodation for hazardous events such as fire, that affect stand productivity (Coops, 1999). Although Healey et al. (2006) found that differences in spectral values for the beginning and end of a prediction period produced smaller RMSEs, we used only basic spectral variables rather than their differences because of mismatches between the years of SNFI field measurements and Landsat acquisition dates for the País Vasco Region (Table 1). For all the models for this Region, only Landsat variables corresponding to the first or final year of an SNFI cycle contributed to statistically significantly improving the quality of fit of the models to the data.

Preliminary analyses showed that the shortwave infrared (SWIR) Landsat B5 was most strongly correlated with forest removals, while NDVI was most strongly correlated with gross annual growth. These results are not unique to this study. For example, Lu et al. (2004) reported a similar relationship between removals and Landsat B5, while Healey et al. (2006) reported a strong relationship between removals and B5 but a weak relationship between removals and NDVI.

4.2. Inference

Hybrid inference is increasingly recognized as the statistically correct approach for estimating the variances of population parameters when only model predictions, rather than observations, are available for a probability sample of population units. Most approaches to hybrid inference have used the model predictions to replace missing observations in the spatial domain (e.g., Ståhl et al., 2011; Gobakken et al., 2012); this is one of only known studies that extend hybrid inference to the temporal domain. Within the hybrid inferential framework, uncertainty from other sources such as allometric model predictions could also be considered (McRoberts et al., 2015, 2016). However, for this study, the effects of allometric model prediction uncertainty on confidence intervals were assumed to have been similar for dataset 2–3 which was used to construct the models and for dataset 3–4 which was used as the source of accuracy assessment data. Therefore, this source of uncertainty would be expected to have no effect on comparisons among methods. Regardless of the domain or the method, the compelling issue is that failure to incorporate the effects of model prediction uncertainty leads to under-estimates of the variance of the population parameter and unduly assessments of precision. When the uncertainty due to the model predictions is small relative to the plot-to-plot variability, the overall effects will also be small. However, when the uncertainty due to the model predictions is of the same order of magnitude as the plot-to-plot variability, then the overall effects are non-negligible as is shown for *Pinus radiata* and *Pinus halepensis* (Table 4).

Finally, we used 4th SNFI estimates of forest type means calculated using only the field observations and simple random sampling (SRS) estimators as standards for comparison. Although the SRS estimator of the mean is unbiased, the estimate obtained for any particular sample could still deviate considerably from the true value. Therefore, our comparisons were based not only on estimated means but also on confidence interval half-widths as quantified by standard errors, $t_{1-\alpha} \cdot SE(\hat{\mu}_4)$. Method C + L produced estimates of means that were more similar to the SRS estimates than did method A. In fact, for two forest types estimates of the means for method A were outside to the confidence intervals for the SRS means. Method A produced the smallest values of $SE(\hat{\mu}_4)$ although the differences between method A and method C + L were small, in absolute terms always less than 0.9 m^3/ha and as a proportion of the SRS values of $SE(\hat{\mu}_4)$ always less than 10%. Therefore, given the considerably greater similarity of method C + L estimates of means to SRS estimates, and only relatively small increases in values of $SE(\hat{\mu}_4)$, method C + L was deemed preferable to the other methods.

4.3. Future investigations

Several issues would benefit from future investigation. First, compensating for the Landsat 7 ETM + sensor malfunctions and/or the unavailability of Landsat 5 TM for some dates by using other sources of spectral data such as MODIS merit consideration (Hayes and Cohen, 2007; Hayes et al., 2008). Second, for method C, techniques such as seemingly unrelated regressions could be used to estimate the parameters of the three models simultaneously with the possibility of increasing overall model prediction accuracies (Vanclay and Skovsgaard, 1997). Third, the effects of uncertainty from additional sources such as allometric model predictions could be incorporated into the analyses. Fourth, it would be interested to extend the current study to other forest conditions including broadleaf forest types, uneven-aged forests, and mixed species conditions.

5. Conclusions

Most European countries use NFI information to respond to the increasing demand for forest information required by international organizations. However, when NFI re-measurement cycles are not synchronized with required reporting frequencies, then if current estimates are to be reported, prediction techniques are required to update both NFI estimates and the accompanying estimates of uncertainty to the reporting years.

We compared five methods for predicting annual, plot-level volume changes as a means of updating growing stock volume estimates. The most accurate method included three models, one for predicting annual gross volume increment, one for predicting the probability of removals, and one for predicting the amount of removals. Moreover, including predictor variables based on the Landsat spectral data increased model prediction accuracy. With this method estimates of mean growing stock volume were the most similar to the simple random sampling estimates based on plot-level observations. Although the relative standard errors with this method were slightly larger than for some other methods, the gain in accuracy offsets the slight loss in precision. For construction of inferences in the form of confidence intervals, hybrid inferential methods were required so that both the model prediction uncertainty and the uncertainty associated with sampling were correctly and statistically rigorously accommodated. Failure to incorporate both sources of uncertainty leads to under-estimates of variances and could lead to poor decisions.

The operational implications of the study were threefold. First, the study demonstrated that countries with established NFIs can accurately and confidently respond to reporting requirements for years for which no field-based survey has yet been conducted. Second, use of Landsat-based metrics as predictor variables in growth models incorporates proxies for ground-level change such as disturbance between surveys. Third, the study demonstrated the operational necessity of accommodating model prediction uncertainty in variance estimators as a means of circumventing undue confidence in estimates. The study also extended these emerging hybrid inferential techniques from the spatial to the temporal domain.

Acknowledgements

The authors thank the Spanish Ministry of Education, Culture and Sports, which partially funded this research through grant PRX16/00180 from the "Salvador de Madariaga" programme.

Appendix A. Supplementary material

Supplementary data associated with this article can be found, in the online version, at http://dx.doi.org/10.1016/j.foreco.2017.04.046.

References

Barreiro, S., Schelhaas, M.-J., Kändler, G., Antón-Fernández, C., Colin, A., Bontemps, J.-D., Alberdi, I., Condés, S., Dumitru, M., Ferezliev, A., Fischer, C., Gasparini, P., Gschwantner, T., Kindermann, G., Kjartansson, B., Kovácsevics, P., Kucera, M., Lundström, A., Marin, G., Mozgeris, G., Nord-Larsen, T., Packalen, T., Redmond, J., Sacchelli, S., Sims, A., Snorrason, A., Stoyanov, N., Thürig, E., Wikberg, P., 2016. Overview of methods and tools for evaluating future woody biomass availability in European countries. Ann. For. Sci. 73, 823–837.

Beauchamp, J.J., Olson, J.S., 1973. Corrections for bias in regression estimates after logarithmic transformation. Ecology, 1403–1407.

Boisvenue, C., Smiley, B.P., White, J.C., Kurz, W.A., Wulder, M.A., 2016. Integration of Landsat time series and field plots for forest productivity estimates in decision support models. For. Ecol. Manage. 376, 284–297.

Cienciala, E., Tomppo, E., Snorrason, A., Broadmeadow, M., Colin, A., Dunger, K., Exnerova, Z., Lasserre, B., Petersson, H., Priwitzer, T., 2008. Preparing emission reporting from forests: use of National Forest Inventories in European countries.

Cohen, W.B., Goward, S.N., 2004. Landsat's role in ecological applications of remote sensing. Bioscience 54, 535–545.

Coops, N., 1999. Improvement in predicting stand growth of Pinus radiata (D. Don) across landscapes using NOAA AVHRR and Landsat MSS imagery combined with a forest growth process model (3-PGS). Photogramm. Eng. Remote Sensing 65, 1149–1156.

Corona, P., Fattorini, L., Franceschi, S., Scrinzi, G., Torresan, C., 2014. Estimation of standing wood volume in forest compartments by exploiting airborne laser scanning information: model-based, design-based, and hybrid perspectives. Can. J. For. Res. 44, 1303–1311.

Efron, B., Tibshirani, R.J., 1994. An Introduction to the Bootstrap. Chapman & Hall/CRC.

Ellis, J., Moarif, S., 2015. Identifying and Addressing Gaps in the UNFCCC Reporting Framework (No. 2015/7). OECD Publishing.

Fridman, J., Holm, S., Nilsson, M., Nilsson, P., Ringvall, A.H., Ståhl, G., 2014. Adapting national forest inventories to changing requirements–the case of the Swedish National Forest Inventory at the turn of the 20th century. Silva Fenn. 48, 1095.

Gobakken, T., Næsset, E., Nelson, R., Bollandsås, O.M., Gregoire, T.G., Ståhl, G., Holm, S., Ørka, H.O., Astrup, R., 2012. Estimating biomass in Hedmark County, Norway using national forest inventory field plots and airborne laser scanning. Remote Sens. Environ. 123, 443–456.

González-Alonso, F., Merino-De-Miguel, S., Roldán-Zamarrón, A., García-Gigorro, S., Cuevas, J., 2006. Forest biomass estimation through NDVI composites. The role of remotely sensed data to assess Spanish forests as carbon sinks. Int. J. Remote Sens. 27, 5409–5415.

Gonzalo Jiménez, J., 2010. Diagnosis fitoclimática de la España Peninsular: hacia un modelo de clasificación funcional de la vegetación y de los ecosistemas peninsulares españoles. Organismo Autónomo de Parques Nacionales.

Goslee, S.C., 2011. Analyzing remote sensing data in R: the landsat package. J. Stat. Softw. 43, 1–25.

Hall, R., Skakun, R., Arsenault, E., Case, B., 2006. Modeling forest stand structure attributes using Landsat ETM+ data: application to mapping of aboveground biomass and stand volume. For. Ecol. Manage. 225, 378–390.

Hayes, D.J., Cohen, W.B., 2007. Spatial, spectral and temporal patterns of tropical forest cover change as observed with multiple scales of optical satellite data. Remote Sens. Environ. 106, 1–16.

Hayes, D.J., Cohen, W.B., Sader, S.A., Irwin, D.E., 2008. Estimating proportional change in forest cover as a continuous variable from multi-year MODIS data. Remote Sens. Environ. 112, 735–749.

Healey, S.P., Yang, Z., Cohen, W.B., Pierce, D.J., 2006. Application of two regression-based methods to estimate the effects of partial harvest on forest structure using Landsat data. Remote Sens. Environ. 101, 115–126.

IGN, 2003. BCN25. Base Cartográfica Numérica 1:25,000. Instituto Geográfico Nacional, Centro Nacional de Información Geográfica, Ministerio de Fomento, Madrid, Spain.

Lu, D., Mausel, P., Brondızio, E., Moran, E., 2004. Relationships between forest stand parameters and Landsat TM spectral responses in the Brazilian Amazon Basin. For. Ecol. Manage. 198, 149–167.

Martin, G.L., 1982. Notes: a method for estimating ingrowth on permanent horizontal sample points. For. Sci. 28, 110–114.

Martonne, E., 1926. Une Nouvelle Fonction Climatologique: L'Indice d'Aridite (A New Climatological Function: The Aridity Index). La Météorologie 2, 449–458.

McRoberts, R.E., 2010. Probability-and model-based approaches to inference for proportion forest using satellite imagery as ancillary data. Rem. Sens. Environ. 114, 1017–1025.

McRoberts, R.E., Chen, Q., Domke, G.M., Ståhl, G., Saarela, S., Westfall, J.A., 2016. Hybrid estimators for mean aboveground carbon per unit area. For. Ecol. Manage. 378, 44–56.

McRoberts, R.E., Næsset, E., Gobakken, T., 2013. Inference for lidar-assisted estimation of forest growing stock volume. Rem. Sens. Environ. 128, 268–275.

McRoberts, R.E., Moser, P., Zimmerman Oliveira, L., Vibrans, A.C., 2015. A general method for assessing the effects of uncertainty in individual-tree volume model predictions on large-area volume estimates with a subtropical forest illustration. Can. J. For. Res. 45, 44–51.

Nabuurs, G.-J., Pussinen, A., Van Brusselen, J., Schelhaas, M., 2007. Future harvesting pressure on European forests. Eur. J. Forest Res. 126, 391–400.

Nagelkerke, N.J., 1991. A note on a general definition of the coefficient of determination. Biometrika 78, 691–692.

Peng, C., 2000. Growth and yield models for uneven-aged stands: past, present and future. For. Ecol. Manage. 132, 259–279.

Ratwosky, D.A., 1983. Nonlinear Regression Modeling. A Unified Practical Approach. Marcel Dekker Inc, New York.

Riaño, D., Chuvieco, E., Salas, J., Aguado, I., 2003. Assessment of different topographic corrections in Landsat-TM data for mapping vegetation types (2003). IEEE Trans. Geosci. Remote Sens. 41, 1056–1061.

Salas-González, R., Houllier, F., Lemoine, B., Pignard, G., 2001. Forecasting wood resources on the basis of national forest inventory data. Application to Pinus pinaster Ait. in southwestern France. Ann. For. Sci. 58, 785–802.

Song, C., Woodcock, C.E., Seto, K.C., Lenney, M.P., Macomber, S.A., 2001. Classification and change detection using Landsat TM data: when and how to correct atmospheric effects? Rem. Sens. Environ. 75, 230–244.

Ståhl, G., Holm, S., Gregoire, T.G., Gobakken, T., Næsset, E., Nelson, R., 2011. Model-based inference for biomass estimation in a LiDAR sample survey in Hedmark County, Norway. Can. J. For. Res. 41, 96–107.

Ståhl, G., Saarela, S., Schnell, S., Holm, S., Breidenbach, J., Healey, S.P., Patterson, P.L., Magnussen, S., Næsset, E., McRoberts, R.E., 2016. Use of models in large-area forest surveys: comparing model-assisted, model-based and hybrid estimation. For. Ecosyst. 3, 5.

Suratman, M., Bull, G., Leckie, D., Lemay, V., Marshall, P., Mispan, M., 2004. Prediction models for estimating the area, volume, and age of rubber (Hevea brasiliensis) plantations in Malaysia using Landsat TM data. Int. Forest. Rev. 6, 12.

Teillet, P., Guindon, B., Goodenough, D., 1982. On the slope-aspect correction of multispectral scanner data. Can. J. Rem. Sens. 8, 84–106.

Tomppo, E., Gschwantner, T., Lawrence, M., McRoberts, R.E., 2010. National Forest Inventories: Pathways for Common Reporting. Springer, Berlin, p. 610.

Tomter, S.M., Kuliešis, A., Gschwantner, T., 2016. Annual volume increment of the European forests—description and evaluation of the national methods used. Ann. For. Sci. 73, 849–856.

Tucker, C.J., 1979. Red and photographic infrared linear combinations for monitoring vegetation. Rem. Sens. Environ. 8, 127–150.

Vanclay, J.K., Skovsgaard, J.P., 1997. Evaluating forest growth models. Ecol. Model. 98, 1–12.

Vidal, C., Alberdi, I., Redmond, J., Vestman, M., Lanz, A., Schadauer, K., 2016. The role of European National Forest Inventories for international forestry reporting. Ann. For. Sci. 73, 793–806.